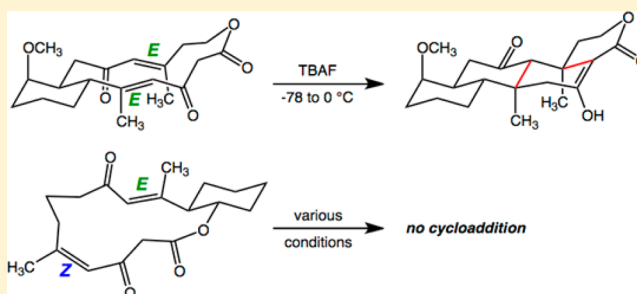


Factors Controlling the Facility of Transannular Diels–Alder Reactions of Macrocyclic Bis-enones

Q. Nhu N. Nguyen,[‡] Jiong Yang,[†] and Dean J. Tantillo^{*,‡}[†]Department of Chemistry, Texas A&M University, College Station, Texas 77843, United States[‡]Department of Chemistry, University of California—Davis, One Shields Avenue, Davis, California 95616, United States

S Supporting Information

ABSTRACT: The reactivity of macrocyclic bis-enones in Diels–Alder reactions was examined using quantum chemical calculations. Stepwise pathways for these transannular cycloaddition reactions were shown to predominate. Steric interactions and torsional strain appeared to play a major role in controlling the overall barrier for polycycle formation.



INTRODUCTION

Inspired by Evans and co-workers' elegant use of a transannular, base-triggered, polycycle-forming oxy-diene + enone Diels–Alder reaction (which can also be formulated as a Michael/Michael cascade reaction) for the total synthesis of salvinorin A,¹ Yang and co-workers explored the feasibility of several transannular Diels–Alder reactions of 14-membered macrocyclic bis-enones to form natural product skeletons containing 6/6/6/6 tetracyclic ring systems (Scheme 1).^{2,3} These bis-enones each possess two C=C π -bonds, allowing for four possible configurations: EE, EZ, ZZ, and ZE. Substrates with each of these configurations were synthesized and then treated with TBAF in THF–DMF (–78–0 °C, 2–3 h).^{2,3} E,Z- and E,E-macrocycles (indicating the configuration of the π -bond nearest to the lactone carbonyl first) cyclized to form diastereomeric products in approximately 90% yield, but Z,E- and Z,Z-macrocycles were either recovered at room temperature or decomposed without cyclization at elevated temperature (Scheme 1). Herein, we describe the results of quantum chemical calculations (using density functional theory) to rationalize the reactivity differences for these bis-enones.

METHODS

Initial optimization and frequency calculations for minima and transition-state structures (TSSs) for macrocyclic bis-enones were carried out using the B3LYP/6-31G(d),⁴ mPW1PW91/6-31+G(d,p),⁵ and M06-2X/6-31+G(d,p)⁶ methods as implemented in Gaussian09.⁷ On the basis of these results, we chose to use M06-2X/6-31+G(d,p) for all subsequent calculations.⁸ Intrinsic reaction coordinate (IRC) calculations were performed for TSSs to confirm the minima to which they are connected (see the Supporting Information for IRC plots).⁹ All calculations were carried out in THF with the SMD solvation model.¹⁰

Conformational searches were carried out with Spartan10 using MM/MMFF with an energy window of 50 kcal/mol.¹¹ Refinement of the lowest energy structures from each conformer library was done

with HF/3-21G followed by M06-2X/6-31+G(d,p) for the lowest energy structures.

¹H and ¹³C chemical shifts in chloroform were predicted using SMD-mPW1PW91/6-311G+(2d,p)//M06-2X/6-31G+(d,p) calculations with scaling factors (slope = –1.0938 for ¹H and –1.0446 for ¹³C; intercept = 31.8723 for ¹H and 186.7246 for ¹³C) applied to convert computed isotropic values into chemical shifts (vs TMS).¹² Boltzmann averaging was used to account for contributions from all conformers that are within 3 kcal/mol (ΔG) of the lowest energy conformer for each system.^{12,13}

RESULTS AND DISCUSSION

For all systems, we searched for the TSSs using both enolate-based dienes (oxy-dienes) and enol-based dienes. All enol–diene substrates were predicted to undergo concerted asynchronous [$\pi_4s + \pi_2s$] Diels–Alder cycloadditions, whereas all enolate–diene substrates were predicted to undergo stepwise cycloadditions (i.e., Michael/Michael reactions; Scheme 2).¹⁴ The carbonyl group adjacent to the dienophile C=C π -bond in each system allows for delocalization of negative charge in the intermediate formed from enolate attack; i.e., a delocalized anion (reactant) is transformed into a different delocalized anion (intermediate). For the enol systems, charge-separated species would be formed from the enol attack (and are found along reaction coordinates; left, center, Scheme 2), but the barriers for these to collapse to products are nonexistent; thus, such intermediates were not located. Overall barriers for concerted cycloadditions of enol-based reactants were predicted to be at least 7 kcal/mol greater than barriers for stepwise cycloadditions of enolate-based reactants. Consequently, enol-based mechanisms were not considered further.

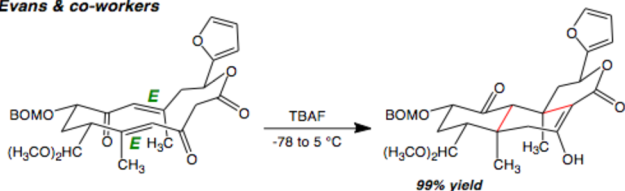
E,Z-Macrocycles. Conformational searches using enolate and enol forms of the E,Z-reactant (Scheme 1) yielded 33 and

Received: June 11, 2014

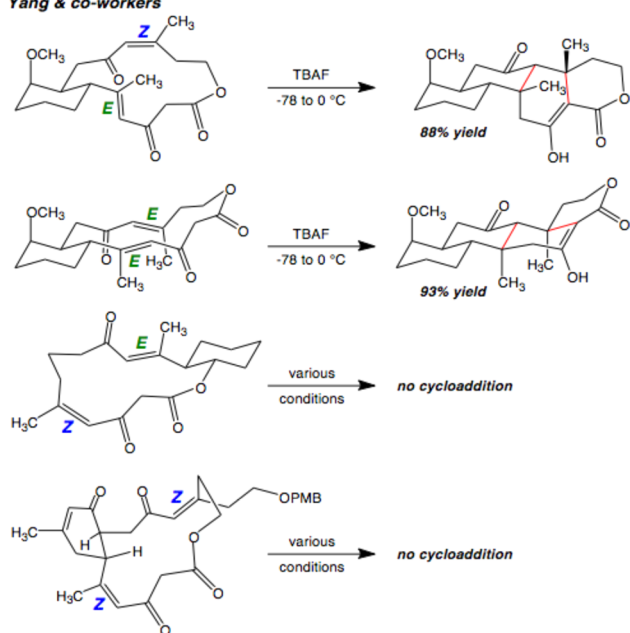
Published: July 7, 2014

Scheme 1. Previous Experimental Work by the Evans and Yang Groups. Bonds Formed in Cycloaddition Steps Are Highlighted in Red

Evans & co-workers



Yang & co-workers



80 possible conformations, respectively. After reoptimization with M06-2X/6-31+G(d,p), complete reaction pathways toward the polycyclic product were determined for the five lowest energy conformers; energies for the three lowest energy unique pathways starting from the enolate forms of the reactants are shown in Table 1. Although **EZ-2-R** was nearly 5 kcal/mol higher in energy than the lowest energy conformer found, **EZ-1-R**, its stepwise conversion to polycyclic product involved the lowest energy rate-determining TSS (Figure 1 and Table 1). The predicted overall barrier for this route (18 kcal/mol relative to enolate reactant **EZ-1-R**) is consistent with a successful reaction under the conditions used experimentally.

In addition, we computed chemical shifts for the keto forms of reactant conformers **EZ-1**, **EZ-2**, and **EZ-3**. **EZ-1-keto-R** remained the lowest energy structure among all the conformers examined (Table 1; enol forms were higher in energy). However, when chemical shifts of **EZ-1-keto-R** were included in the averaging to predict the experimental chemical shifts, the match between theory and experiment was not as good as when taking into account only **EZ-2-keto-R** and structures less than 1 kcal/mol from it. Boltzmann averaging of **EZ-1-keto-R**, **EZ-2-keto-R**, and **EZ-3-keto-R** yielded mean absolute deviations (MADs) between experimental and theoretical chemical shifts of 0.2 for ^1H and 2.5 for ^{13}C , whereas Boltzmann averaging of only **EZ-2-keto-R** and **EZ-3-keto-R** yielded MADs of 0.2 for ^1H and 2.1 for ^{13}C . This suggests that **EZ-1** may not be among the experimentally observed reactant conformers. This would be possible if the macrocycle-forming synthetic step produces **EZ-2** selectively and **EZ-1** and **EZ-2** do not interconvert. A

Scheme 2. Possible Reaction Mechanisms (Illustrated for the *E,Z* Macrocyclic Bis-enones from Scheme 1)

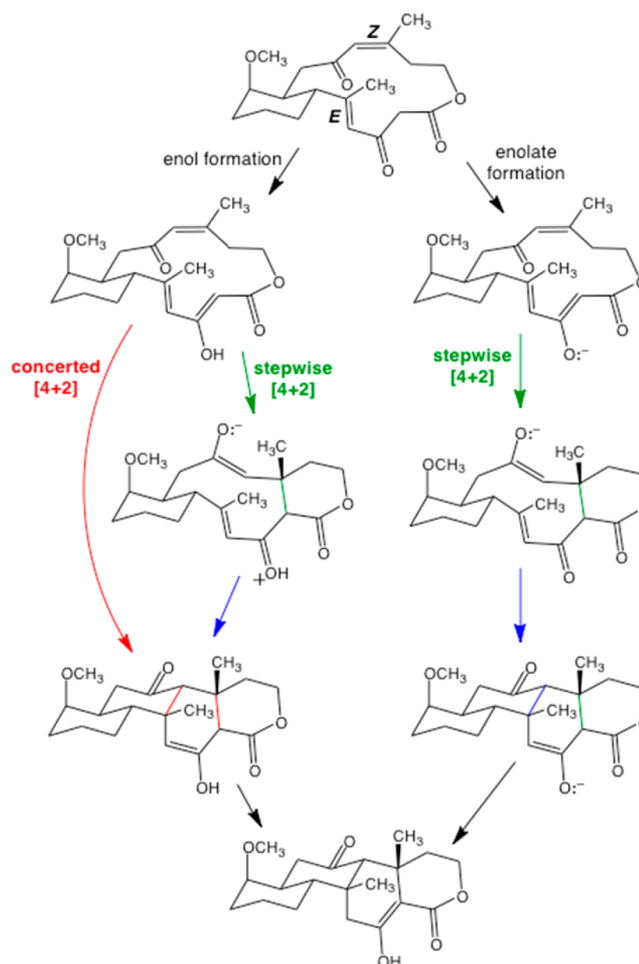


Table 1. Relative ΔG 's (kcal/mol) for Relevant Conformers of *E,Z*-Macrocyclic and Their Respective TSSs and Minima^a

	keto-R	R (enolate)	TS1	Int	TS2	P
EZ-1	0.0	0.0	15.0	0.8	27.2	23.7
EZ-2	2.5	4.7	18.3	4.4	13.4	-4.1
EZ-3	3.3	1.6	17.4	3.6	19.5	2

^aKeto energies are relative to the lowest energy keto conformer; all other energies are relative to the lowest energy enolate conformer.

conformer resembling **EZ-2** was found in the solid state,³ but the relevance of this observation to solution phase behavior is not clear-cut. Although our computational evidence is circumstantial at best, if this scenario does occur, the barrier for polycycle formation will be lowered considerably.

***E,E*-Macrocycles.** Conformational searches using enolate and enol forms of the *E,E*-reactant yielded 55 and 27 possible conformations, respectively. After reoptimization with M06-2X/6-31+G(d,p), complete reaction pathways toward the polycyclic product were determined for the three lowest energy enolate conformers and six lowest energy enol conformers (all other conformers found were approximately 10 or more kcal/mol higher than the lowest energy conformer for each protonation state), but none of these pathways were energetically viable.

Consequently, we performed an additional conformational search using the TSS for the first C–C bond formation step

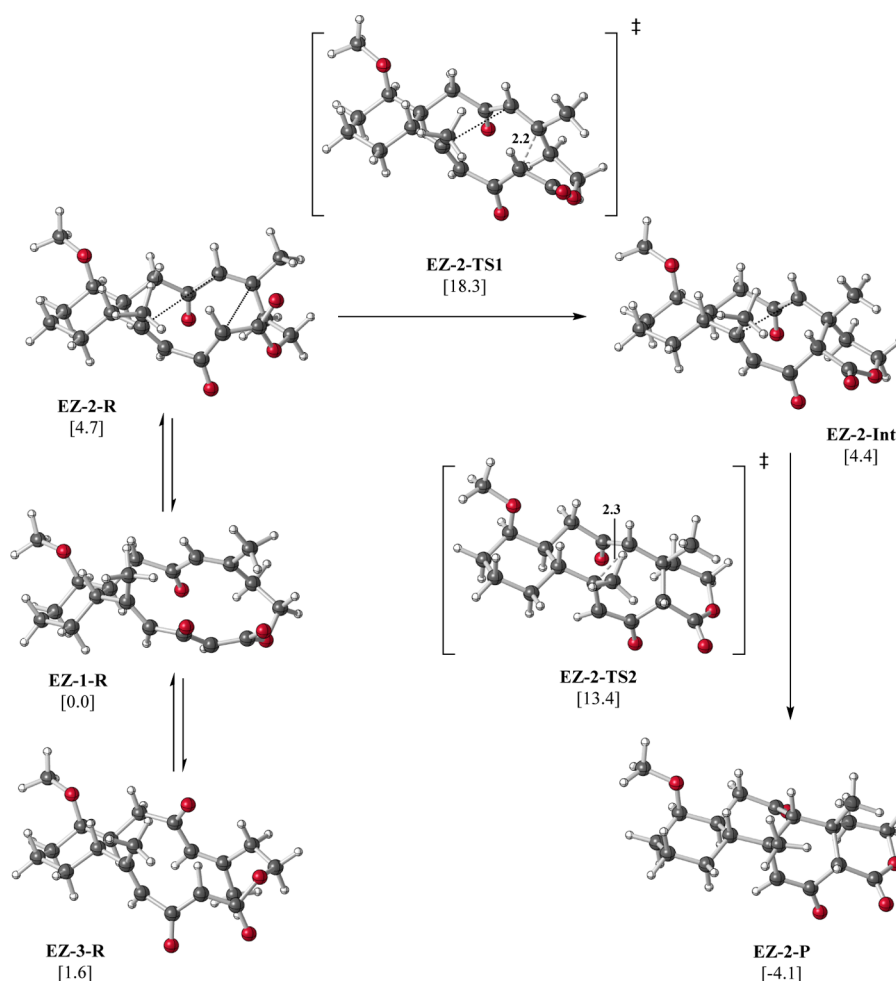


Figure 1. Reaction pathway for EZ-2 starting from the enolate form of the reactant. Relative ΔG 's are shown in kcal/mol, and selected distances are shown in Å.

from the enolate pathways that looked most promising, obtaining 45 conformations that were then optimized to TSSs with B3LYP/6-31G(d) and, subsequently, M06-2X/6-31+G(d,p). Complete pathways leading to the polycyclic product using the five lowest energy TSSs were then mapped out; energies for the three lowest energy unique pathways are shown in Table 2. EE-1-R (Figure 2) was the lowest energy enolate

Table 2. Relative ΔG 's (kcal/mol) for Relevant Conformers of *E,E*-Macrocyclic and Their Respective TSSs and Minima^a

	keto-R	R (enolate)	TS1	Int1/Int2	TS2	P
EE-1	4.2	0.0	18.2	10.5/23	32.9	10.5
EE-2	8.8	7.9	22.4	8.6	19.4	-7.8
EE-3	0.5	3.1	23.5		33.2	

^aNote that two intermediates (different conformers) are found for the pathway from EE-1. Keto energies are relative to the lowest energy keto conformer; all other energies are relative to the lowest energy enolate conformer.

reactant and also was connected to the lowest energy TSS for initial C–C bond formation (Table 2). However, its second TSS was too high in energy for this pathway to be productive (Table 2). EE-2-R was predicted to follow the most energetically feasible route, with an overall predicted barrier of 22 kcal/mol, relative to the energy of EE-1-R (Figure 2 and Table 2).

This barrier is higher than one would expect for a facile reaction under the conditions used (Scheme 1), so we wondered if the preferred reaction might start from EE-1-R and proceed through EE-1-TS1 to EE-1-Int, which might interconvert with EE-2-Int so as to allow access to the lower energy EE-2-TS2. Unfortunately, the TSS associated with the interconversion of EE-1-Int and EE-2-Int was predicted to be 21.5 kcal/mol above the energy of EE-1-R.

We then ran three additional conformational searches starting with the lowest energy conformations found for EE-TS1, EE-TS2, and EE-Int, obtaining 37, 61, and 30 conformers for each, respectively. Unfortunately, none of the pathways associated with any of these structures had lower overall barriers than the pathway corresponding to reactant EE-2-R.

These results led us to consider the possibility that conformer EE-2-R is formed during the synthesis of EE-2 and does not convert to EE-1-R. If this were the case, the overall barrier from EE-2-R to the cycloaddition product would be only 14.5 kcal/mol. We predicted the chemical shifts for the *E,E*-macrocyclic in its keto-form, and the predicted chemical shifts for the lowest energy conformer found, EE-3-keto-R (Table 2), were a slightly better match to the experimental shifts (MADs of 0.13 for ¹H and 1.97 for ¹³C) than those for EE-1-keto-R (MADs of 0.12 for ¹H and 2.08 for ¹³C) or EE-2-keto-R (MADs of 0.14 for ¹H and 3.10 for ¹³C). While these results are inconclusive, we note that not converting

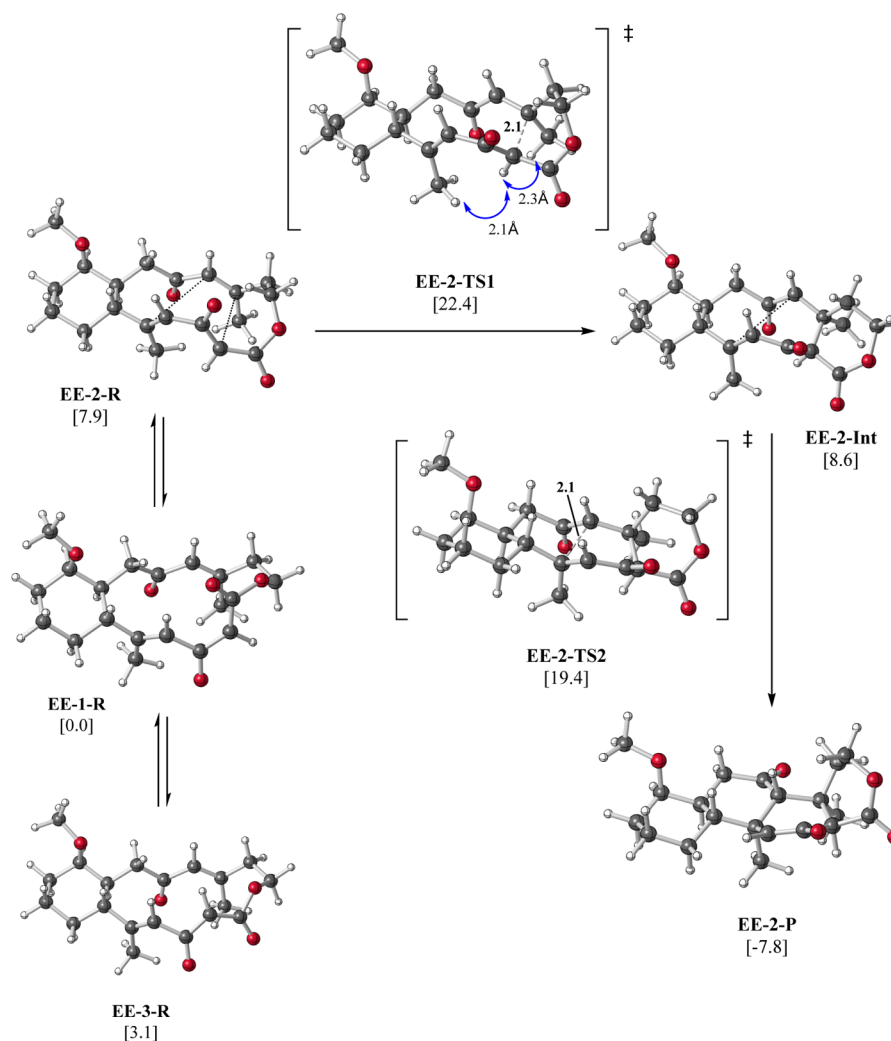


Figure 2. Reaction pathway for EE-2 starting from the enolate form of the reactant. Relative ΔG^\ddagger 's are shown in kcal/mol, and selected distances are shown in Å.

between the lowest energy conformer, EE-3-keto-R, and EE-1-keto-R (precursor to the lowest energy enolate conformer) would lead to lowering of the energy barrier by approximately 3 kcal/mol.

Z,E-Macrocycles. A conformational search on the keto-form of the cyclohexane-fused Z,E-macrocyclic used in the experimental study (Scheme 1) resulted in 59 conformers, and complete reaction pathways were determined for two *s-trans* dienolate conformers and one *s-cis* dienolate conformers, all derived from the lowest energy keto conformers by deprotonation and reoptimization. A separate conformational search was carried out using the latter TSS, which yielded 20 conformers. The pathway starting from the enolate conformer ZE-2-R has the lowest overall barrier among all the pathways that were examined (Figure 3 and Table 3). However, this predicted barrier, 25.6 kcal/mol from ZE-2-R and 28.5 kcal/mol from the preferred ZE-1-R (Figure 3), is higher than those for the E,E and E,Z macrocycles, high enough that we would predict that this reaction would not occur under the experimental conditions used (a free energy of activation of approximately 20 kcal/mol or less is expected for a successful reaction), which was indeed experimentally observed. As shown in Figure 3, significant steric clashes are present in the high energy TSS (hydrogens 1.8 or 2.1 Å apart), interactions that are intensified

as the TSS is reached. In addition, the bond angles involving the carbon atoms of the (Z) C=C bond both expand further from the ideal trigonal planar angle as the TSS is formed.

Comparing experimental and computed chemical shifts for this Z,E-macrocyclic was more challenging because clear peak assignments for all protons in the experimental spectrum were not available. Nonetheless, most of the computed values fell within the proposed experimental ranges. Once again, there was no strong evidence to support that the particular conformer(s) formed synthetically was unable to interconvert with other conformers (see the Supporting Information for details).

Z,Z-Macrocycles. Next, we examined a Z,Z-macrocyclic with a structure the same as that examined experimentally, except that the OPMP group was replaced by a methoxy group in our calculations (Figure 4). A conformational search using the keto-form of the reactant yielded 100 conformers. After deprotonation and reoptimization, complete reaction pathways were calculated for the three lowest energy conformers (all being *s-trans*) along with the three lowest energy *s-cis* conformers. A separate conformational search using the lowest-energy *s-cis* TS1 was also carried out, resulting in 18 conformers. Again, a high barrier (28 kcal/mol) was found for the lowest energy pathway (Figure 4 and Table 4). As illustrated in Figure 4, steric clashes are again present in the highest energy TSS (hydrogens 1.8 Å

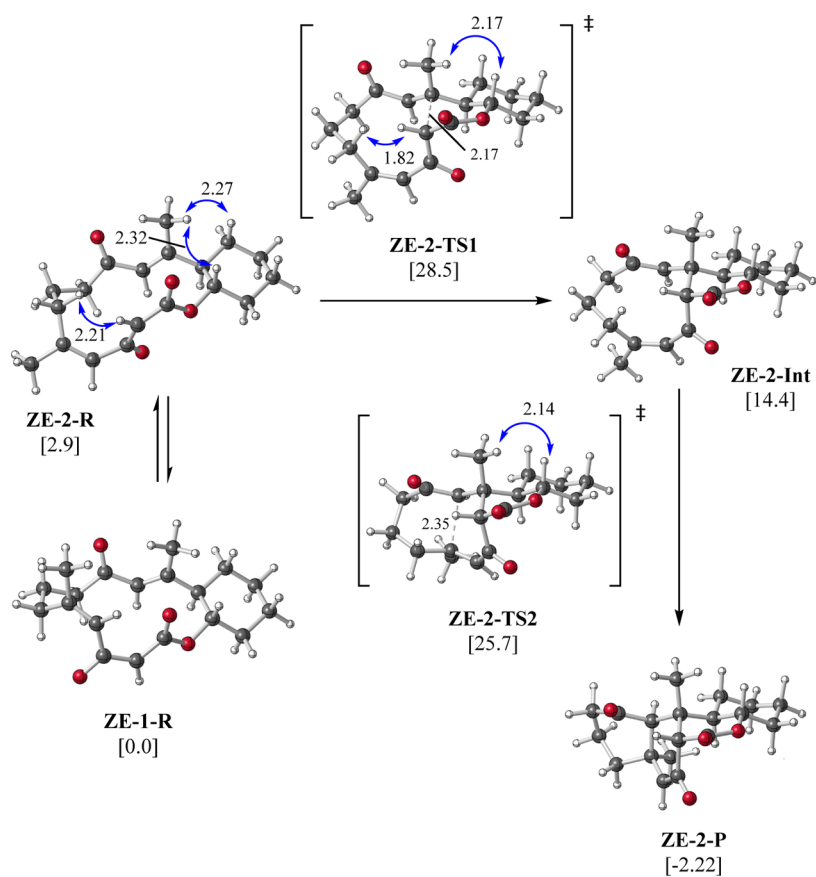


Figure 3. Reaction pathway for ZE-2 starting from the enolate form of the reactant. Relative ΔG^\ddagger 's are shown in kcal/mol, and selected distances are shown in Å.

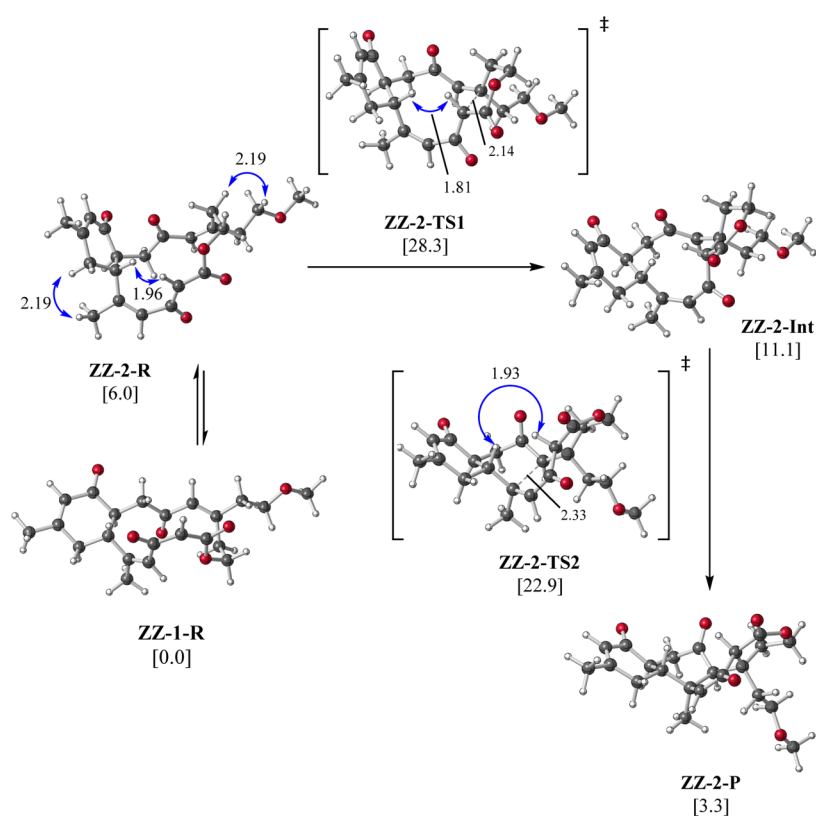


Figure 4. Reaction pathway for ZZ-2 starting from the enolate form of the reactant. Relative ΔG^\ddagger 's are shown in kcal/mol, and selected distances are shown in Å.

Table 3. Relative ΔG 's (kcal/mol) for Relevant Conformers of Z,E-Macrocycles and Their Respective TSSs and Minima^a

	keto-R	R (enolate)	TS1	Int	TS2	P
ZE-1	0.00	0.0	27.2	14.3	43.9	4.6
ZE-2	6.5	2.9	28.5	14.4	25.7	-2.22

^aKeto energies are relative to the lowest energy keto conformer; all other energies are relative to the lowest energy enolate conformer.

Table 4. Relative ΔG 's (kcal/mol) for Relevant Conformers of Z,Z-Macrocycles and Their Respective TSSs and Minima^a

	keto-R	R (enolate)	TS1	Int	TS2	P
ZZ-1	2.0	0.0	27.9	10.0	33.1	25.2
ZZ-2	0.0	6.0	28.3	11.1	22.9	3.3

^aKeto energies are relative to the lowest energy keto conformer; all other energies are relative to the lowest energy enolate conformer.

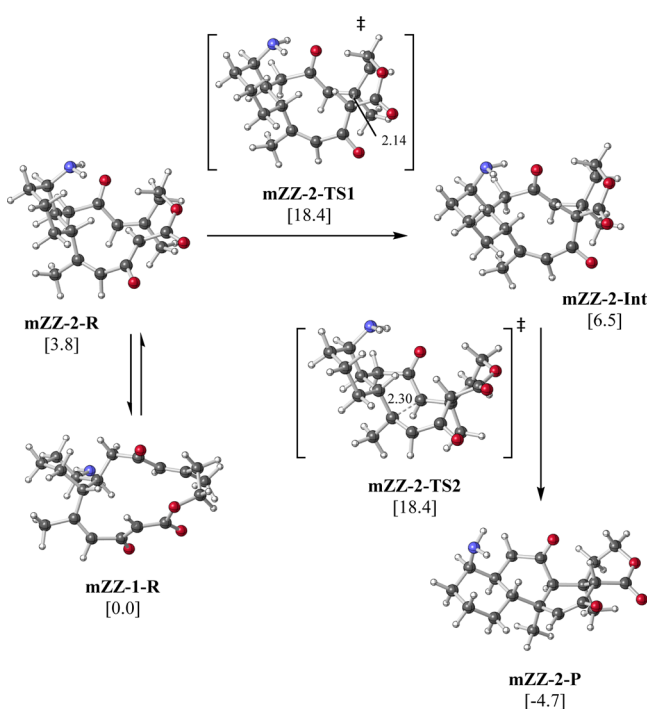


Figure 5. Reaction pathway for modified Z,Z-macrocycle starting from the enolate form of the reactant. Relative ΔG 's are shown in kcal/mol, and selected distances are shown in Å.

apart); angle strain associated with the (Z) C=C bond again increases as this TSS is reached as well. Once again, there was no strong evidence to support that the particular conformer(s) formed synthetically was unable to interconvert with other conformers (see the Supporting Information for details).

Modifying the Z,Z-Macrocycle. For comparison, the Z,Z-isomer of the methoxycyclohexane-fused bis-enones described above was also examined computationally (this system was not studied experimentally).¹⁵ The overall predicted barrier for this system (25 kcal/mol) again indicated that such reaction is not likely. Comparing the two Z,Z-macrocyclic systems indicated that the fused ring affected the energy barriers. The flexibility of the methoxycyclohexane compared with the cyclohexanone seemed to allow the macrocycle to adjust its conformation to reduce steric interactions during bond formation. Consequently, we examined replacement of the methoxy group with an amine to allow for hydrogen bonding between the amine and carbonyl,

an interaction that would predispose the macrocycle to adopt a productive conformation and activate the dienophile. For this new Z,Z-system, we performed a conformational search using the first TSS as input geometry, resulting in 31 conformers (the best are shown in Figure 5). We computed reaction pathways for the four lowest energy TSS conformers. Indeed, our calculations indicated that the overall energy barrier for cyclization was lowered to around 18 kcal/mol. Although an amine group may not be the best choice synthetically for such a reaction, the effect described here provides a model for rationally facilitating an otherwise unfavorable cycloaddition.

CONCLUSIONS

The results of our calculations indicate that stepwise Diels–Alder processes (Michael/Michael reactions) are favored for all of the macrocyclic bis-enones examined. We predict overall cycloaddition barriers of 18 and 22 kcal/mol for the two bis-enones that react experimentally but barriers of 28–29 kcal/mol for the two bis-enones that do not react experimentally. Steric and strain effects hinder reaction of the latter two bis-enones. A means for lowering these barriers is proposed.

ASSOCIATED CONTENT

Supporting Information

Coordinates and energies for all computed structures, IRC plots, additional conformational search information, computed ¹H and ¹³C NMR data, and full Gaussian citation. This material is available free of charge via the Internet at <http://pubs.acs.org>.

AUTHOR INFORMATION

Corresponding Author

*E-mail: djtantillo@ucdavis.edu.

Notes

The authors declare no competing financial interest.

ACKNOWLEDGMENTS

This work was supported in part by the National Science Foundation (CHE-1150606 to J.Y. and supercomputing resources through a grant from the XSEDE program: CHE-030089 to D.J.T.) and the Robert A Welch Foundation (A-1700). We also thank Ryan Pemberton for many helpful discussions.

REFERENCES

- (1) Scheerer, J. R.; Lawrence, J. F.; Wang, G. C.; Evans, D. A. *J. Am. Chem. Soc.* **2007**, *129*, 8968–8969.
- (2) Xue, H.; Yang, J.; Gopal, P. *Org. Lett.* **2011**, *13*, 5696–5699.
- (3) Xue, H.; Gopal, P.; Yang, J. *J. Org. Chem.* **2012**, *77*, 8933–8945.
- (4) (a) Becke, A. D. *Phys. Rev. A* **1988**, *38*, 3098–3100. (b) Lee, C.; Yang, W.; Parr, R. G. *Phys. Rev. B* **1988**, *37*, 785–789. (c) Miehlich, B.; Savin, A.; Stoll, H.; Preuss, H. *Chem. Phys. Lett.* **1989**, *157*, 200–206.
- (5) (a) Adamo, C.; Barrone, V. J. *Chem. Phys.* **1998**, *108*, 664–675. (b) *Electronic Structure of Solids '91* Perdew, J. P.; Ziesche, P., Eschrig, H., Eds.; Akademie Verlag: Berlin, 1991; p 11.
- (6) Zhao, Y.; Truhlar, D. G. *Theor. Chem. Acc.* **2008**, *120*, 215–241.
- (7) Gaussian 09, Revision B.01; Gaussian, Inc.: Wallingford, CT, 2004 (full reference in the Supporting Information).
- (8) Energy barriers computed with B3LYP were 3–13 kcal/mol higher than those computed with M06-2X. mPW1PW91 barriers were approximately 3 kcal/mol lower than those from M06-2X in general (see the Supporting Information).
- (9) (a) Fukui, K. *Acc. Chem. Res.* **1981**, *14*, 363–368. (b) Gonzalez, C.; Schlegel, H. B. *J. Phys. Chem.* **1990**, *94*, 5523–5527.
- (10) Marenich, A. V.; Cramer, C. J.; Truhlar, D. G. *J. Phys. Chem. B* **2009**, *113*, 6378–6396.

- (11) *Spartan'10*, Wavefunction, Inc.: Irvine, CA, 2010.
- (12) (a) Lodewyk, M. W.; Siebert, M. R.; Tantillo, D. J. *Chem. Rev.* **2012**, *112*, 1839–1862. (b) Jain, R.; Bally, T.; Rablen, P. R. *J. Org. Chem.* **2009**, *74*, 4017–4023. (c) CHESHIRE, Chemical Shift Repository with Coupling Constants Added Too. <http://cheshirenmr.info>, accessed 7/14/14.
- (13) Lodewyk, M. W.; Tantillo, D. J. *J. Nat. Prod.* **2011**, *74*, 1339–1343.
- (14) All minima featured in the discussed pathways were obtained by optimizing the last points of IRC calculations from associated TSSs.
- (15) The *Z,E* analogue was also examined. See the Supporting Information for details.